OPEN ACCESS Freely available online

PLOS ONE

Effect of Joule Heating and Thermal Radiation in Flow of Third Grade Fluid over Radiative Surface

Tasawar Hayat[1,2], Anum Shafiq[1]*, Ahmed Alsaedi[2]

1 Department of Mathematics, Quaid-i-Azam University, Islamabad, Pakistan, **2** Nonlinear Analysis and Applied Mathematics (NAAM) Research Group, Faculty of Science, King Abdulaziz University, Jeddah, Saudi Arabia

Abstract

This article addresses the boundary layer flow and heat transfer in third grade fluid over an unsteady permeable stretching sheet. The transverse magnetic and electric fields in the momentum equations are considered. Thermal boundary layer equation includes both viscous and Ohmic dissipations. The related nonlinear partial differential system is reduced first into ordinary differential system and then solved for the series solutions. The dependence of velocity and temperature profiles on the various parameters are shown and discussed by sketching graphs. Expressions of skin friction coefficient and local Nusselt number are calculated and analyzed. Numerical values of skin friction coefficient and Nusselt number are tabulated and examined. It is observed that both velocity and temperature increases in presence of electric field. Further the temperature is increased due to the radiation parameter. Thermal boundary layer thickness increases by increasing Eckert number.

Citation: Hayat T, Shafiq A, Alsaedi A (2014) Effect of Joule Heating and Thermal Radiation in Flow of Third Grade Fluid over Radiative Surface. PLoS ONE 9(1): e83153. doi:10.1371/journal.pone.0083153

Editor: Vanesa Magar, Plymouth University, United Kingdom

Received July 30, 2013; **Accepted** October 30, 2013; **Published** January 15, 2014

Funding: This paper was funded by the Deanship of Scientific Research (DSR), King Abdulaziz University, Jeddah under grant no. (10-130/1433 HiCi). The funders had no role in study design, data collection and analysis, decision to publish, or preparation of the manuscript.

Competing Interests: The authors have declared that no competing interests exist.

* E-mail: anumshafiq@ymail.com

Introduction

There is a substantial interest of the recent researchers in the flows of non-Newtonian fluids. Such motivation in these fluids is mainly because of their use in the industrial and technological applications. Many materials like mud, pasta, personal care products, ice cream, paints, oils, cheese, asphalt etc. are non-Newtonian fluids. Most biological fluids with higher molecular weight components are also non-Newtonian in nature. The usual properties of polymer melts and solutions together with the desirable attributes of many polymeric solids, have given rise to the world-wide industry of polymer processing. The non-Newtonian fluids in particular have key importance in geophysics, chemical and nuclear industries, material processing, oil reservoir engineering, bioengineering and many others. Rheological properties of all the non-Newtonian fluids cannot be predicted using single constitutive equation (unlike the case of viscous fluids). Therefore many models of non-Newtonian fluids are based either on "natural" modifications of established macroscopic theories or molecular considerations. The additional rheological parameter in the constitutive equations of non-Newtonian fluids are the main culprit for the lack of analytical solutions. The resulting equations are more complex and higher order than the Navier-Stokes equations. Hence these equations have been attracted from modelling as well as solutions point of view. The advancement in the study of non-Newtonian fluids has been made even by the recent investigators (See [1–10] and many studies therein).

The flow induced over a stretching surface is very well documented problem in fluid mechanics. It is encountered in extrusion of polymer sheet from a die, glass fiber and paper production, continuous casting, cooling of metallic plate in a bath etc. Such flow problem in presence of heat transfer has been attracted by the researchers due to its applications in polymer processing technology. The quality of end product in industry depends upon both the stretching and cooling rates. Further, the thermal radiation effect has pivotal role in nuclear plants, gas turbines and devices for satellites, space vehicles, aircraft etc. The literature on this topic is quite sizeable. Rana and Bhargava [11] presented the numerical analysis for heat transfer of nanofluid over a nonlinearly stretching sheet. Bhattacharyya et al. [12] analyzed the solutions of boundary layer flow of viscoelastic fluid and heat transfer over a stretching sheet with internal heat generation or absorption. Makinde and Aziz [13] numerically studied the boundary layer flow of viscous nanofluid bounded by a stretching sheet. They considered the transport equation which includes the effects of Brownian motion and thermophoresis. Mandal and Mukhopadhyay [14] considered the boundary layer flow and heat transfer towards an exponentially stretching porous sheet embedded in a porous medium with variable surface heat flux. They found that the momentum and thermal boundary layer thickness decrease with increasing exponential parameter. Hayat et al. [15] examined the heat transfer in flow of second grade fluid over a stretching sheet. Thermal radiation effect in the boundary layer flow by stretching surface has been explored by Sajid and Hayat [16]. Bhattacharyya [17] discussed the unsteady stagnation point flow towards a stretching surface. Effect of heat transfer in flow over an exponentially stretching surface has been explored by Mukhopadhyay [18]. The radiation effect in flow of micropolar fluid towards a stretching surface is addressed by Hussain et al. [19]. Rashidi et al. [20] developed approximate solutions for heat transfer analysis in flow of micropolar fluid. Moreover, the interest

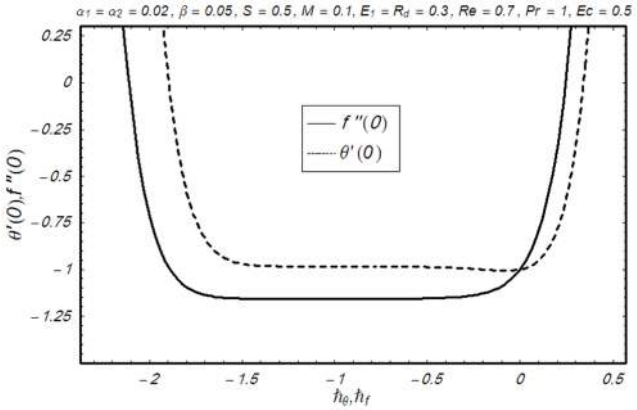

Figure 1. ħ-curves of the functions f″(0) and θ′(0) at 10th order of approximation.
doi:10.1371/journal.pone.0083153.g001

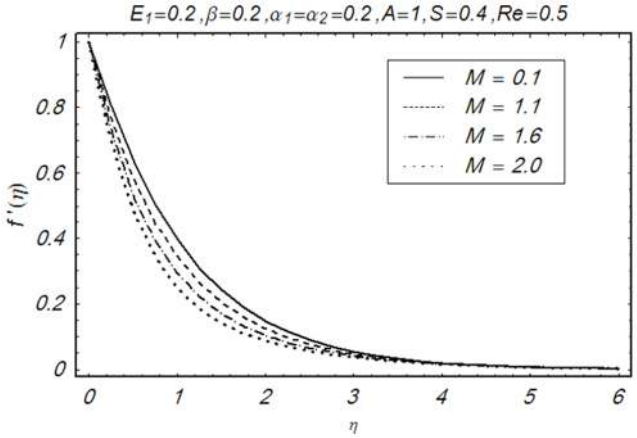

Figure 2. Influence of M on f′(η).
doi:10.1371/journal.pone.0083153.g002

in the study of magnetohydrodynamic flow for an electrically conducting fluid over heated surface is motivated by its great value in a wide range of engineering problems such as plasma studies, petroleum industries, MHD power generators, cooling of nuclear reactors, the boundary layer control in aerodynamics and crystal growth. Hence Turkyilmazoglu [21] found exact solution for magnetohydrodynamic flow of viscous fluid due to a rotating disk. Hayat and Nawaz [22] has investigated the Soret and Dufour effects in mixed convection three dimensional boundary flow of an electrically conducting second grade fluid over a vertical stretching sheet. Ahmad and Nazar [23] considered the problem of unsteady magnetohydrodynamic viscoelastic fluid flowing towards a stagnation point on a vertical surface. Pal and Mondal [24] discussed the hydromagnetic flow of viscous fluid over a stretching surface in presence of both electric and magnetic fields. Abel et al. [25] presented MHD flow analysis for viscoelastic fluid. Both viscous and Ohmic dissipations are presented in this attempt. More, the analysis here is made when magnetic and electric fields are present. Hayat and Qasim [26] considered radiation effect in MHD flow of second grade fluid over unsteady porous stretching surface. The effect of internal heat generation in hydromagnetic non-Darcy flow and heat transfer over a stretching surface with thermal radiation and Ohmic dissipation is examined by Olanrewaju [27]. Elbashbeshy et al. [28] numerically analyzed the problem of unsteady laminar two-dimensional MHD boundary layer flow and heat transfer of an incompressible viscous fluid over a porous surface in the presence of thermal radiation and internal heat generation or absorption. MHD flow caused by a rotating disk is presented by Rashidi et al. [29]. The well-known Jeffery-Hamel problem in presence of magnetic field is examined by Motsa et al. [30]. Most of the studies on MHD flow over a stretching surface with heat transfer do not take into account the effect of electric field and Ohmic dissipation. Very little exists yet about such aspects in the stretched flows of viscous fluids. Such consideration further narrowed down when non-Newtonian fluids have been considered. To our knowledge there is only one such attempt for viscoelastic fluid [25]. The fluid employed although exhibits the normal stress effects but it cannot describe the features of shear thinning or shear thickening. Having such in view, the flow of third grade fluid is considered. This fluid even can capture shear thinning/shear thickening effects for one-dimensional flow over a rigid surface. The main objective here is to analyze the two-dimensional flow of third grade fluid over an unsteady stretching sheet. The effects of both electric and magnetic fields are retained in the momentum and energy equations. Thermal radiation and Ohmic dissipation are taken into account. The solutions for velocity component and temperature are developed by homotopy analysis method (HAM) [31–40]. The plots of physical quantities of interest reflecting the novel features of embedded parameters in the problems are given and analyzed. Tables for skin friction

Table 1. Convergence of homotopy solutions when $\alpha_1 = 0.02$, $\beta = 0.05$, $\alpha_2 = 0.02$, $S = 0.2$, $A = 0.5$, $E_1 = 0.3$, $\mathrm{Re} = 0.7$, $R_1 = 0.3$, $M = 0.1$, $\mathrm{Pr} = 1$, $Ec = 0.5$.

Order of approximation	$-f''(0)$	$-\theta'(0)$
1	1.0419	1.0059
2	1.0720	1.0079
5	1.1210	1.0041
10	1.1442	0.99450
12	1.1458	0.99211
14	1.1458	0.99051
40	1.1458	0.99051

doi:10.1371/journal.pone.0083153.t001

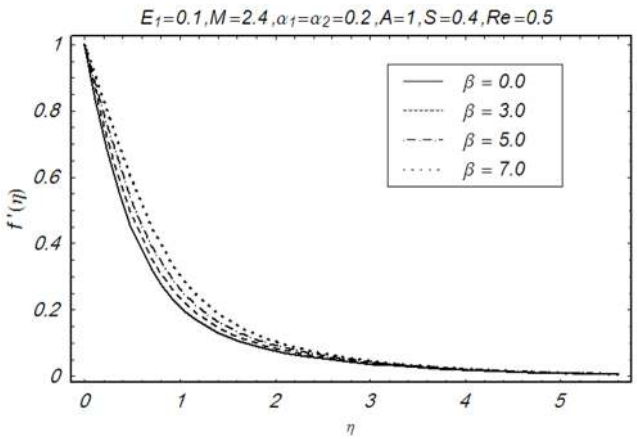

Figure 3. Influence of β on f′(η).
doi:10.1371/journal.pone.0083153.g003

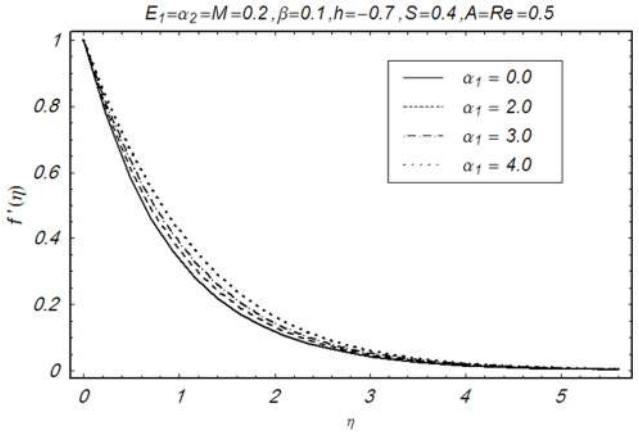

Figure 4. Influence of α_1 on $f'(\eta)$.
doi:10.1371/journal.pone.0083153.g004

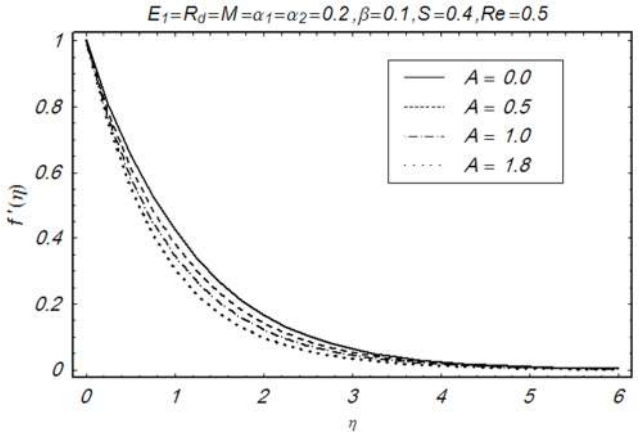

Figure 6. Influence of A on $f'(\eta)$.
doi:10.1371/journal.pone.0083153.g006

coefficient and local Nusselt number are made and explained carefully.

Mathematical Formulation

We examine the two-dimensional boundary layer flow of magnetohydrodynamic (MHD) third grade fluid over a porous stretching surface. Here the fluid is electrically conducting in the presence of applied magnetic $\vec{B}=(0,B_0,0)$ and electric $\vec{E}=(0,0,-E_0)$ fields. The flow is because of stretching of sheet from a slit through two equal and opposite forces. The sheet velocity is taken linear parallel to the flow direction. The electric and magnetic fields obey the Ohm's law $\vec{\mathbf{J}}=\sigma\left(\vec{E}+\vec{V}\times\vec{B}\right)$. Here $\vec{\mathbf{J}}$ is the Joule current, σ is the electrical conductivity and $\vec{V}$ is the fluid velocity. The induced magnetic field and Hall current effects are ignored subject to small magnetic Reynolds number. Both the electric and magnetic fields contribute into the momentum and thermal boundary layer equations. The relevant equations in the aforestated conditions can be expressed as follows:

$$\frac{\partial u}{\partial x}+\frac{\partial v}{\partial y}=0, \tag{1}$$

$$\frac{\partial u}{\partial t}+u\frac{\partial u}{\partial x}+v\frac{\partial u}{\partial y}=$$
$$v\frac{\partial^2 u}{\partial y^2}+\frac{\alpha_1^*}{\rho}\left[\frac{\partial^3 u}{\partial t\partial y^2}+u\frac{\partial^3 u}{\partial x\partial y^2}+v\frac{\partial^3 u}{\partial y^3}+\frac{\partial u}{\partial x}\frac{\partial^2 u}{\partial y^2}+3\frac{\partial u}{\partial y}\frac{\partial^2 u}{\partial x\partial y}\right] \tag{2}$$
$$+2\frac{\alpha_2^*}{\rho}\frac{\partial u}{\partial y}\frac{\partial^2 u}{\partial x\partial y}+6\frac{\beta_3}{\rho}\left(\frac{\partial u}{\partial y}\right)^2\frac{\partial^2 u}{\partial y^2}+\frac{\sigma}{\rho}\left(E_0B_0-B_0^2u\right),$$

$$\rho c_p\left(\frac{\partial T}{\partial t}+u\frac{\partial T}{\partial x}+v\frac{\partial T}{\partial y}\right)=$$
$$K\frac{\partial^2 T}{\partial y^2}+\mu\left(\frac{\partial u}{\partial y}\right)^2+\alpha_1^*\left[\frac{\partial u}{\partial y}\frac{\partial^2 u}{\partial t\partial y}+u\frac{\partial u}{\partial y}\frac{\partial^2 u}{\partial x\partial y}+v\frac{\partial u}{\partial y}\frac{\partial^2 u}{\partial y^2}\right] \tag{3}$$
$$+2\beta_3\left(\frac{\partial u}{\partial y}\right)^4+\sigma(uB_0-E_0)^2-\frac{\partial q_r}{\partial y}.$$

In above equations u and v denote the velocity components in the x and y directions, α_1^*, α_2^* and β_3 are the fluid parameters, ν is the kinematic viscosity, ρ is the density of fluid, T is the fluid temperature, K is the thermal conductivity of fluid, c_p is the

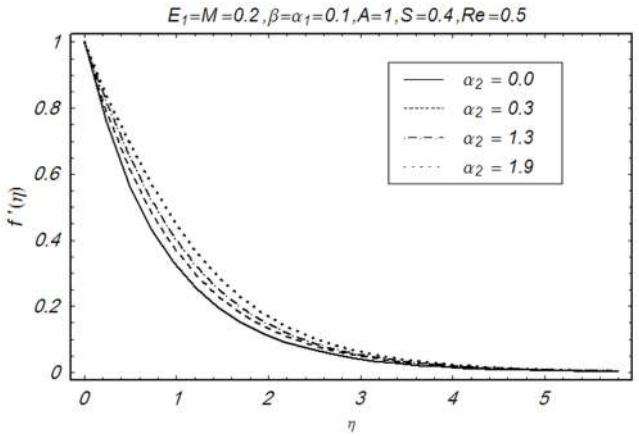

Figure 5. Influence of α_2 on $f'(\eta)$.
doi:10.1371/journal.pone.0083153.g005

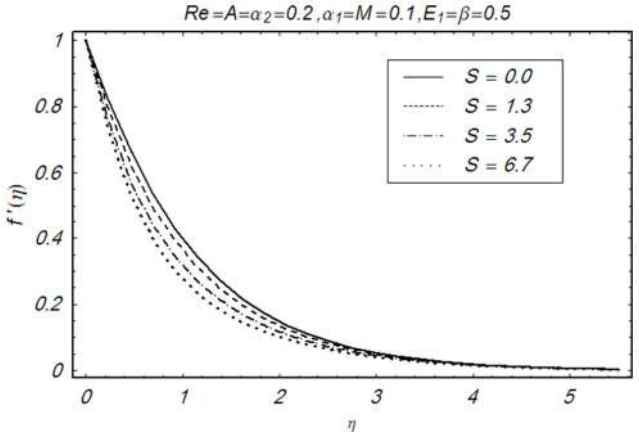

Figure 7. Influence of S on $f'(\eta)$.
doi:10.1371/journal.pone.0083153.g007

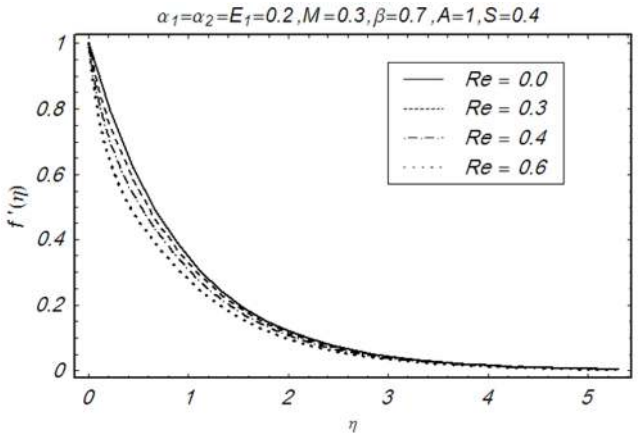

Figure 8. Influence of Re on f′(η).
doi:10.1371/journal.pone.0083153.g008

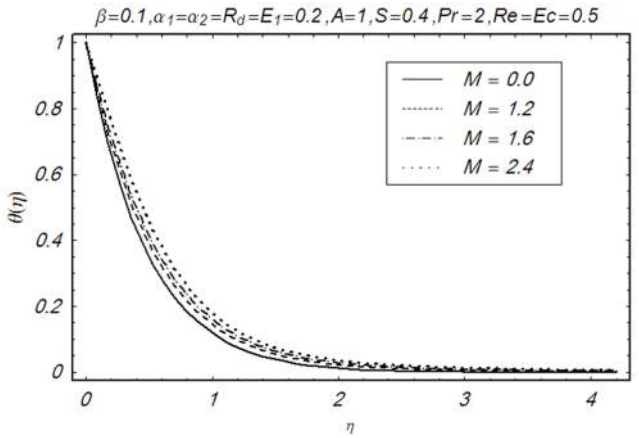

Figure 10. Influence of M on θ(η).
doi:10.1371/journal.pone.0083153.g010

specific heat at constant pressure and the radiative heat flux q_r is first given by Sparrow and Cess [41] and Raptis [42]

$$q_r = -\frac{4\sigma^*}{3k_1}\frac{\partial T^4}{\partial y}, \tag{4}$$

where σ^* is the Stefan-Boltzmann constant and k_1 is the mean absorption coefficient. Through expansion of $T^4 \cong 4T_\infty^3 T - 3T_\infty^4$, Eq. (3) becomes

$$\rho c_p\left(\frac{\partial T}{\partial t}+u\frac{\partial T}{\partial x}+v\frac{\partial T}{\partial y}\right)=\left(\frac{16\sigma^* T_\infty^3}{3k_1}+K\right)\frac{\partial^2 T}{\partial y^2}+\mu\left(\frac{\partial u}{\partial y}\right)^2 + \alpha_1^*\left[\frac{\partial u}{\partial y}\frac{\partial^2 u}{\partial t\partial y}+u\frac{\partial u}{\partial y}\frac{\partial^2 u}{\partial x\partial y}+v\frac{\partial u}{\partial y}\frac{\partial^2 u}{\partial y^2}\right]+2\beta_3\left(\frac{\partial u}{\partial y}\right)^4 + \sigma(uB_0-E_0)^2. \tag{5}$$

The subjected conditions can be mentioned as follows:

$$u(x,0)=U_w,\ v(x,0)=V_w,\ T(x,0)=T_w,$$

$$u\to 0,\quad T\to T_\infty,\quad \text{as}\quad y\to\infty, \tag{6}$$

with V_w defined by

$$V_w = -\frac{v_0}{(1-ct)^{1/2}}. \tag{7}$$

Here the mass transfer at surface with $V_w<0$ is for injection and $V_w>0$ for suction. Also the stretching velocity $U_w(x,t)$ and the surface temperature $T_w(x,t)$ are taken in the forms:

$$U_w(x,t)=\frac{ax}{1-ct},\ T_w(x,t)=T_\infty+T_0\frac{ax}{2v(1-ct)^2}, \tag{8}$$

where a and c are the constants with $a>0$ and $c\geq 0$ (i.e $ct<1$).

If ψ is the stream function then defining

$$\eta=\sqrt{\frac{U_w}{xv}}y,\ \psi=\sqrt{vxU_w}f(\eta),\ \theta=\frac{T-T_\infty}{T_w-T_\infty}, \tag{9}$$

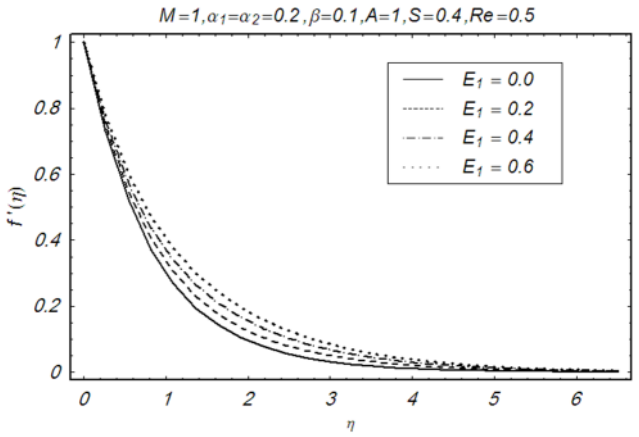

Figure 9. Influence of E_1 on f′(η).
doi:10.1371/journal.pone.0083153.g009

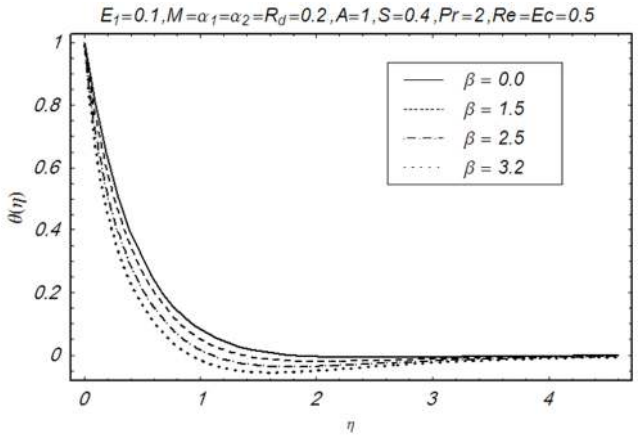

Figure 11. Influence of β on θ(η).
doi:10.1371/journal.pone.0083153.g011

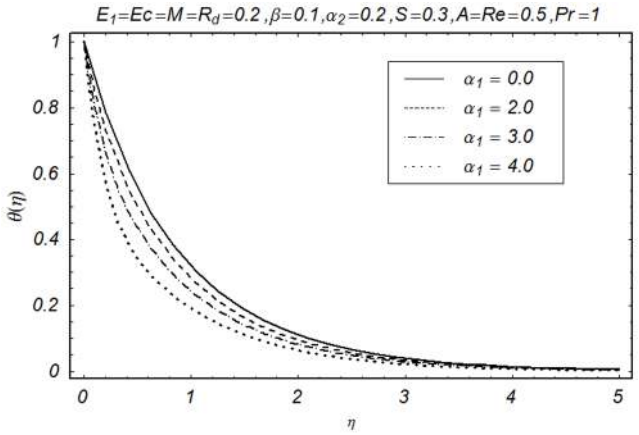

Figure 12. Influence of α_1 on $\theta(\eta)$.
doi:10.1371/journal.pone.0083153.g012

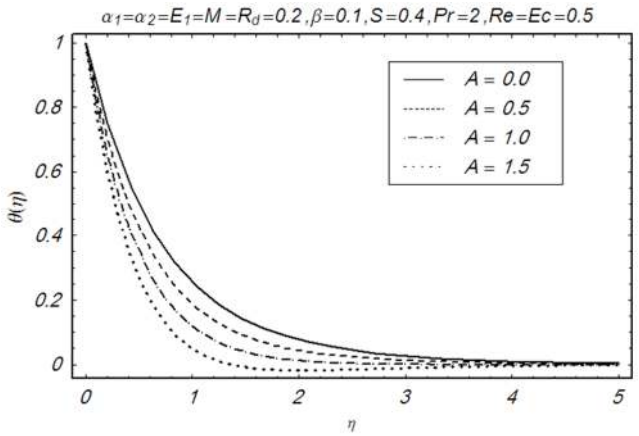

Figure 14. Influence of A on $\theta(\eta)$.
doi:10.1371/journal.pone.0083153.g014

$$u=\frac{\partial\psi}{\partial y},\ v=-\frac{\partial\psi}{\partial x}. \tag{10}$$

The incompressibility condition is identically satisfied and the resulting problems for f and θ are reduced into the following forms

$$\begin{aligned} &f'''+ff''-f'^2-S\left\{f'+\frac{1}{2}\eta f''\right\}+\alpha_1\left[2f'f'''-ff^{(iv)}+3f''^2\right.\\ &\left.+S\left\{2f'''+\frac{1}{2}\eta f^{(iv)}\right\}\right]+2\alpha_2 f''^2+6\beta\,\mathrm{Re}\,f''^2f'''\\ &+M^2\{E_1-f'\}=0\Big), \end{aligned} \tag{11}$$

$$\begin{aligned} &\left(1+\frac{4}{3}R_d\right)\theta''-\mathrm{Pr}\left[f'\,\theta-f\,\theta'+\frac{S}{2}\{\eta\theta'+4\theta\}\right]+\mathrm{Pr}\,Ec\,f''^2\\ &+\alpha_1\,\mathrm{Pr}\,Ec\left[f'f''^2+\frac{S}{2}\{3f''^2+\eta f''f'''\}-ff''f'''\right]\\ &+2\beta\,\mathrm{Pr}\,Ec\,\mathrm{Re}\,f''^4+M^2\,\mathrm{Pr}\,Ec[f'-E_1]^2=0,\Big) \end{aligned} \tag{12}$$

$$f(0)=A, f'(0)=1, f'(\infty)\to 0,\quad f''(\infty)\to 0,\quad \theta(0)=1,\quad \theta(\infty)\to 0, \tag{13}$$

with

$$\begin{aligned} &\mathrm{Re}=\frac{ax^2}{v(1-ct)},\quad M^2=\frac{\sigma B_0^2(1-ct)}{\rho a},\quad E_1=\frac{E_0(1-ct)}{B_0 ax},\\ &\alpha_1=\frac{\alpha_1^* a}{\mu(1-ct)},\quad \alpha_2=\frac{\alpha_2^* a}{\mu(1-ct)},\quad \beta=\frac{\beta_3 a^2}{\mu(1-ct)^2},\\ &A=\frac{v_0}{\sqrt{av}},\quad S=\frac{c}{a},\quad R_d=\frac{4\sigma^* T_\infty^3}{k^* K},\quad \mathrm{Pr}=\frac{\mu c_p}{K},\\ &Ec=\frac{U_w^2}{c_p(T_w-T_\infty)}. \end{aligned} \tag{14}$$

Here Re denotes the Reynolds number, M the magnetic parameter, E_1 is the electric parameter, α_1 and α_2 and β are the fluid parameters, A is the suction parameter, S is the unsteadiness parameter, R_d is the radiation parameter, Pr is the Prandtl number and Ec is the Eckert number.

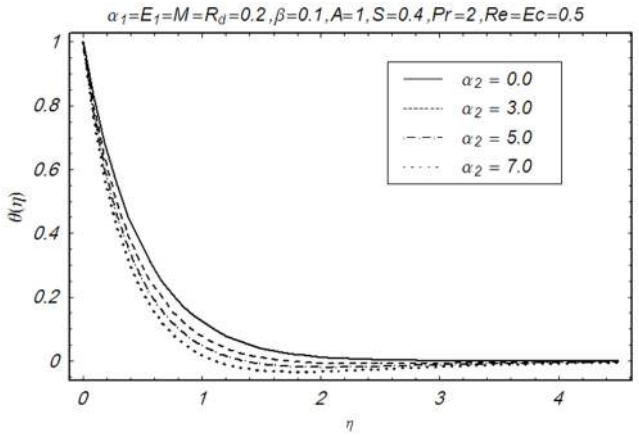

Figure 13. Influence of α_2 on $\theta(\eta)$.
doi:10.1371/journal.pone.0083153.g013

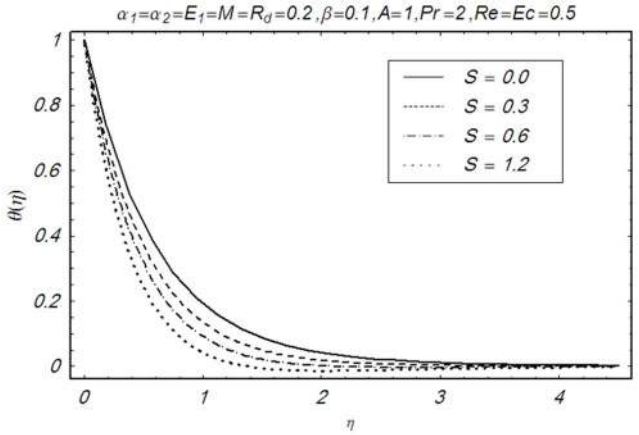

Figure 15. Influence of S on $\theta(\eta)$.
doi:10.1371/journal.pone.0083153.g015

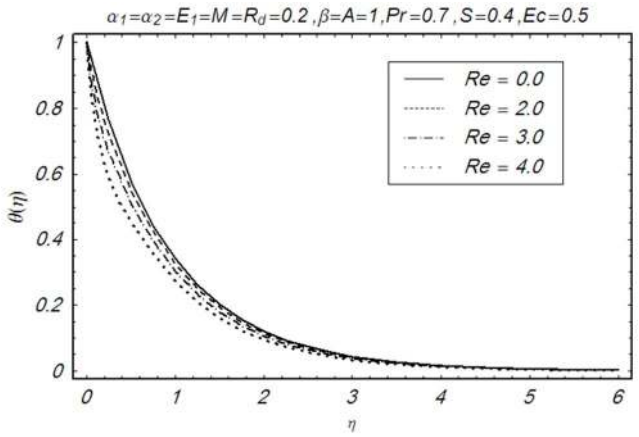

Figure 16. Influence of Re on θ(η).
doi:10.1371/journal.pone.0083153.g016

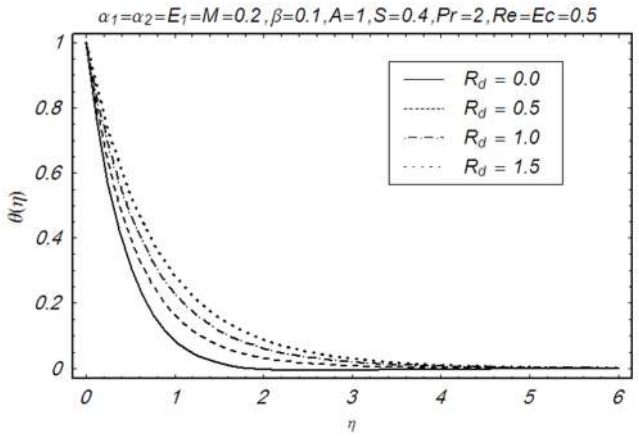

Figure 17. Influence of R_d on θ(η).
doi:10.1371/journal.pone.0083153.g017

The local skin friction coefficient is defined as

$$C_f = \frac{\tau_w}{\rho U_w^2} = \frac{\tau_{xy}\big|_{y=0}}{\rho U_w^2}$$
$$\mathrm{Re}_x^{1/2} C_f = \left[\begin{matrix} f''(0) + \alpha_1 \left\{ 3\tfrac{S}{2} f''(0) + 3f''(0) - Sf'''(0) \right\} \\ + 2\beta\, \mathrm{Re} f''^3(0) \end{matrix} \right]. \quad (15)$$

The Nusselt number is given by

$$Nu_x = \frac{x q_w}{K(T_w - T_\infty)} = \frac{x\left(K + \dfrac{16\sigma^* {T_\infty}^3}{3k_1}\right)\dfrac{\partial T}{\partial y}\Big|_{y=0}}{K(T_w - T_\infty)}$$

$$\mathrm{Re}_x{}^{-1/2} Nu_x = -\left(1 + \frac{4}{3} R_d\right)\theta'(0), \quad (16)$$

in which $\mathrm{Re}_x = \dfrac{ax^2}{v(1-ct)}$ is the local Reynolds number.

Solutions

The velocity and temperature can be expressed in the set of base functions

$$\left\{ \eta^k \exp(-n\eta) \middle| k \geq 0, n \geq 0 \right\} \quad (17)$$

can be expressed as follows

$$f(\eta) = a_{0,0}^0 + \sum_{n=0}^{\infty} \sum_{k=0}^{\infty} a_{m,n}^k \eta^k \exp(-n\eta), \quad (18)$$

$$\theta(\eta) = \sum_{n=0}^{\infty} \sum_{k=0}^{\infty} b_{m,n}^k \eta^k \exp(-n\eta), \quad (19)$$

where $a_{m,n}^k$ and $b_{m,n}^k$ are the coefficients.

The initial guesses f_0 and θ_0 in homotopy solutions are taken through the expressions

$$f_0(\eta) = A + 1 - \exp(-\eta),\ \theta_0(\eta) = \exp(-\eta). \quad (20)$$

The auxiliary linear operators and their associated properties are

$$\mathbf{L}(f) = \frac{d^3 f}{d\eta^3} - \frac{df}{d\eta}, \quad \mathbf{L}(\theta) = \frac{d^2\theta}{d\eta^2} - \theta, \quad (21)$$

satisfy the following properties

$$\mathbf{L}_f[C_1 + C_2 \exp(\eta) + C_3 \exp(-\eta)] = 0, \quad (22)$$

$$\mathbf{L}_\theta[C_4 \exp(\eta) + C_5 \exp(-\eta)] = 0, \quad (23)$$

Where $C_i (i = 1-5)$ depict the arbitrary constants.

The zeroth order problems are

$$(1-p)\mathbf{L}_f[\hat{f}(\eta,p) - f_0(\eta)] = p\hbar_f \mathbf{N}_f\left[\hat{f}(\eta,p)\right],$$
$$(1-p)\mathbf{L}_\theta[\hat{\theta}(\eta,p) - \theta_0(\eta)] = p\hbar_\theta \mathbf{N}_\theta\left[\hat{f}(\eta,p), \hat{\theta}(\eta,p)\right], \quad (24)$$

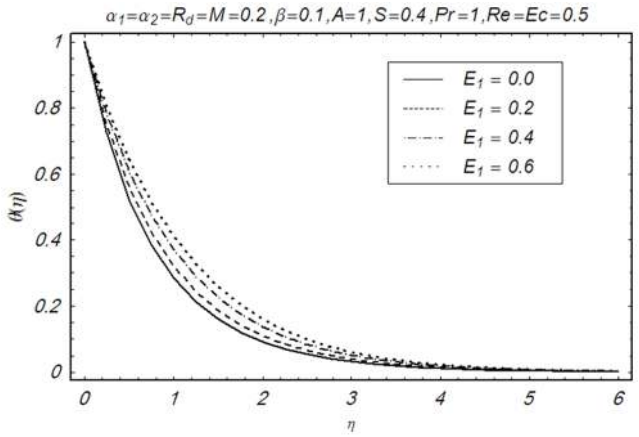

Figure 18. Influence of E_1 on θ(η).
doi:10.1371/journal.pone.0083153.g018

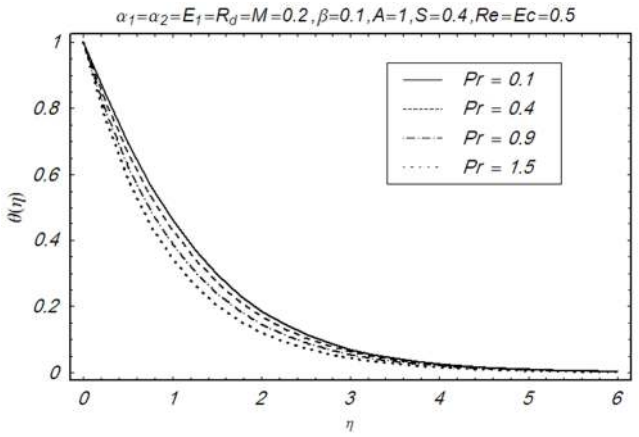

Figure 19. Influence of Pr on θ(η).
doi:10.1371/journal.pone.0083153.g019

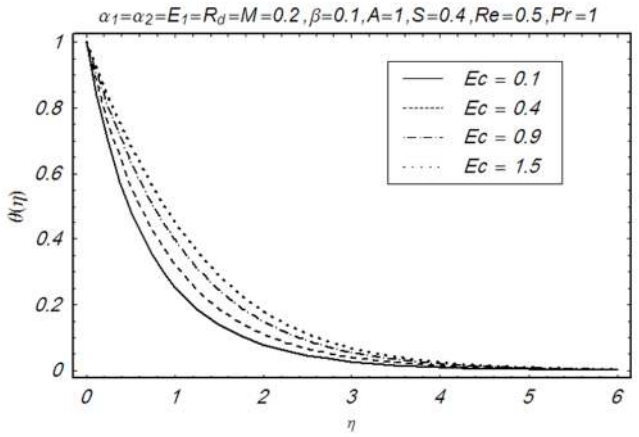

Figure 20. Influence of Ec on θ(η).
doi:10.1371/journal.pone.0083153.g020

$$\hat{f}(\eta;\, p)\Big|_{\eta=0}=A,\ \frac{\partial\hat{f}'(\eta;\, p)}{\partial\eta}\Big|_{\eta=0}=1,\ \frac{\partial\hat{f}'(\eta;\, p)}{\partial\eta}\Big|_{\eta=\infty}=0,$$
$$\hat{\theta}(\eta;\, p)\Big|_{\eta=0}=1,\ \hat{\theta}(\eta;\, p)\Big|_{\eta=\infty}=0, \tag{25}$$

with non-linear operators $\mathbf{N}_f\left[\hat{f}(\eta,p)\right]$ and $\mathbf{N}_\theta\left[\hat{f}(\eta,p),\hat{\theta}(\eta,p)\right]$ defined by

$$N_f\left[\hat{f}(\eta;\, p)\right]=\frac{\partial^3\hat{f}(\eta,p)}{\partial\eta^3}+\hat{f}(\eta,p)\frac{\partial^2\hat{f}(\eta,p)}{\partial\eta^2}-\left(\frac{\partial\hat{f}(\eta,p)}{\partial\eta}\right)^2$$
$$-S\left\{\frac{\partial\hat{f}(\eta,p)}{\partial\eta}+\frac{1}{2}\eta\frac{\partial^2\hat{f}(\eta;\, q)}{\partial\eta^2}\right\}+\alpha_1\left\{2\frac{\partial\hat{f}(\eta,p)}{\partial\eta}\frac{\partial^3\hat{f}(\eta;\, q)}{\partial\eta^3}\right.$$
$$-\hat{f}(\eta,p)\frac{\partial^4\hat{f}(\eta,p)}{\partial\eta^4}+S\left\{2\frac{\partial^3\hat{f}(\eta;\, q)}{\partial\eta^3}+\frac{1}{2}\eta\frac{\partial^4\hat{f}(\eta,p)}{\partial\eta^4}\right\}+ \tag{26}$$
$$\left.3\left(\frac{\partial^2\hat{f}(\eta,p)}{\partial\eta^2}\right)^2\right\}+2\alpha_2\left(\frac{\partial^2\hat{f}(\eta,p)}{\partial\eta^2}\right)^2+6\beta\,\mathrm{Re}\left(\frac{\partial^2\hat{f}(\eta,p)}{\partial\eta^2}\right)^2$$
$$\frac{\partial^3\hat{f}(\eta;\, q)}{\partial\eta^3}+M^2\left\{E_1-\frac{\partial\hat{f}(\eta,p)}{\partial\eta}\right\},$$

$$N_\theta\left[\hat{f}(\eta;\, p),\hat{\theta}(\eta;\, p)\right]=\left(1+\frac{4}{3}R_d\right)\frac{\partial^2\hat{\theta}(\eta;\, p)}{\partial\eta^2}+\mathrm{Pr}\,Ec\left(\frac{\partial^2\hat{f}(\eta,p)}{\partial\eta^2}\right)^2$$
$$-\mathrm{Pr}\left[\frac{S}{2}\left\{4\theta+\eta\frac{\partial\hat{\theta}(\eta;\, p)}{\partial\eta}\right\}+\frac{\partial\hat{f}(\eta;\, q)}{\partial\eta}\hat{\theta}(\eta;\, p)-\hat{f}(\eta,p)\frac{\partial\hat{\theta}(\eta;\, p)}{\partial\eta}\right]$$
$$+\alpha_1\,\mathrm{Pr}\,Ec\left[\frac{S}{2}\left\{3\left(\frac{\partial^2\hat{f}(\eta,p)}{\partial\eta^2}\right)^2+\eta\frac{\partial^2\hat{f}(\eta,p)}{\partial\eta^2}\frac{\partial^3\hat{f}(\eta;\, q)}{\partial\eta^3}\right\}\right. \tag{27}$$
$$+\frac{\partial\hat{f}(\eta;\, q)}{\partial\eta}\left(\frac{\partial^2\hat{f}(\eta,p)}{\partial\eta^2}\right)^2-\hat{f}(\eta,p)\frac{\partial^2\hat{f}(\eta,p)}{\partial\eta^2}\frac{\partial^3\hat{f}(\eta;\, q)}{\partial\eta^3}\Bigg]$$
$$+2\beta\,\mathrm{Pr}\,Ec\,\mathrm{Re}\left(\frac{\partial^2\hat{f}(\eta;\, q)}{\partial\eta^2}\right)^4+M^2\,\mathrm{Pr}\,Ec\left[\frac{\partial\hat{f}(\eta;\, q)}{\partial\eta}-E_1\right]^2,$$

in which $p\in[0,1]$ indicates the embedding parameter and h_f and h_θ the nonzero auxiliary parameters.

Setting $p=0$ and $p=1$ we have

$$\hat{f}(\eta;\, 0)=f_0(\eta),\quad \hat{\theta}(\eta;\, 0)=\theta_0(\eta),$$
$$\hat{f}(\eta;\, 1)=f(\eta),\quad \hat{\theta}(\eta;\, 1)=\theta(\eta). \tag{28}$$

When p increases from 0 to 1, $\hat{f}(\eta;\, p)$ and $\hat{\theta}(\eta;\, p)$ deforms from the initial solutions $f_0(\eta)$ and $\theta_0(\eta)$ to the final solutions $f(\eta)$ and $\theta(\eta)$, respectively. Taylor series, of $\hat{f}(\eta;\, p)$ and $\hat{\theta}(\eta;\, p)$ gives

$$\hat{f}(\eta;\, p)=f_0(\eta)+\sum_{m=1}^{\infty}f_m(\eta)p^m,\qquad f_m(\eta)=\frac{1}{m!}\frac{\partial^m\hat{f}(\eta;\, p)}{\partial p^m}\Big|_{p=0},$$
$$\hat{\theta}(\eta;\, p)=\theta_0(\eta)+\sum_{m=1}^{\infty}\theta_m(\eta)p^m,\qquad \theta_m(\eta)=\frac{1}{m!}\frac{\partial^m\hat{\theta}(\eta;\, p)}{\partial p^m}\Big|_{p=0}. \tag{29}$$

The auxiliary parameters are properly chosen such that the series solutions converge at $p=1$. Therefore

$$f(\eta)=f_0(\eta)+\sum_{m=1}^{\infty}f_m(\eta),\ \theta(\eta)=\theta_0(\eta)+\sum_{m=1}^{\infty}\theta_m(\eta). \tag{30}$$

The mth-order deformation problems are

$$\mathrm{L_f}[\mathrm{f_m}(\eta)-\chi_\mathrm{m}\mathrm{f_{m-1}}(\eta)]=\hbar_\mathrm{f}\mathrm{R_m^f}(\eta),\ \mathrm{L_\theta}[\theta_\mathrm{m}(\eta)-\chi_\mathrm{m}\theta_\mathrm{m-1}(\eta)]=$$
$$\hbar_\theta\mathrm{R_m^\theta}(\eta), \tag{31}$$

$$\hat{f}_m(\eta;\, p)\Big|_{\eta=0}=0,\ \frac{\partial\hat{f}_m'(\eta;\, p)}{\partial\eta}\Big|_{\eta=0}=0,\ \frac{\partial\hat{f}_m'(\eta;\, p)}{\partial\eta}\Big|_{\eta=\infty}=0,$$
$$\hat{\theta}_m(\eta;\, p)\Big|_{\eta=0}=0,\ \hat{\theta}_m(\eta;\, p)\Big|_{\eta=\infty}=0, \tag{32}$$

Table 2. Numerical values of skin friction coefficients $\mathrm{Re}_x^{1/2}C_f$ for different values of physical parameters.

α_1	α_2	β	S	M	E_1	Re	$-\mathrm{Re}_x^{1/2}C_f$
0.00	0.1	0.2	0.5	0.1	0.3	0.7	1.453
0.10							1.532
0.14							1.567
0.1	0.0	0.2	0.5	0.1	0.3	0.7	1.600
	0.1						1.632
	0.2						1.668
0.1	0.1	0.0	0.5	0.1	0.3	0.7	1.433
		0.1					1.489
		0.2					1.532
0.1	0.1	0.2	0.5	0.1	0.3	0.7	1.532
			0.6				1.592
			0.7				1.670
0.1	0.1	0.2	0.5	0.1	0.3	0.7	1.532
				0.2			1.536
				0.3			1.545
0.01	0.01	0.2	0.5	0.1	0.5	0.7	1.492
					0.6		1.487
					0.7		1.482
0.1	0.1	0.2	0.5	0.1	0.3	0.7	1.532
						0.8	1.542
						0.9	1.551

doi:10.1371/journal.pone.0083153.t002

$$\begin{aligned}\mathrm{R}_{\mathrm{m}}^{\mathrm{f}}(\eta)&=f_{m-1}^{'''}(\eta)+\sum_{k=0}^{m-1}\left(f_{m-1-k}f_{k}^{''}-f_{m-1-k}^{'}f_{k}^{'}\right)-\\&S\left(f_{m-1}^{'}+\frac{1}{2}\eta f_{m-1}^{''}\right)+\sum_{k=0}^{m-1}\alpha_1\left[2f_{m-1-k}^{'}f_{k}^{'''}-f_{m-1-k}f_{k}^{(iv)}\right.\\&\left.+3f_{m-1-k}^{''}f_{k}^{''}\right]+\alpha_1 S\left\{2f_{m-1}^{'''}+\frac{1}{2}\eta f_{m-1}^{(iv)}\right\}+2\alpha_2\sum_{k=0}^{m-1}f_{m-1-k}^{''}f_{k}^{''}\\&+6\beta\,\mathrm{Re}\sum_{k=0}^{m-1}f_{m-1-k}^{''}\sum_{l=0}^{k}f_{k-l}^{''}f_{l}^{'''}+M^2\left[E_1(1-\chi_m)-f_{m-1}^{'}\right],\end{aligned}\tag{33}$$

$$\begin{aligned}\mathrm{R}_{\mathrm{m}}^{\theta}(\eta)&=\left(1+\frac{4}{3}R_d\right)\theta_{m-1}^{''}\\&-\mathrm{Pr}\left[\sum_{k=0}^{m-1}f_{m-1-k}^{'}\theta_k-\sum_{k=0}^{m-1}f_{m-1-k}\theta_{k}^{'}+\frac{S}{2}\left\{\eta\theta_{m-1}^{'}+4\theta_{m-1}\right\}\right]\\&+\mathrm{Pr}\,Ec\sum_{k=0}^{m-1}f_{m-1-k}^{''}f_{k}^{''}+\alpha_1\,\mathrm{Pr}\,Ec\left[\sum_{k=0}^{m-1}f_{m-1-k}^{'}\sum_{l=0}^{k}f_{k-l}^{''}f_{l}^{''}\right.\\&\left.+\frac{S}{2}\sum_{k=0}^{m-1}\left\{3f_{m-1-k}^{''}f_{k}^{''}+\eta f_{m-1-k}^{''}f_{k}^{'''}\right\}-\sum_{k=0}^{m-1}f_{m-1-k}\sum_{l=0}^{k}f_{k-l}^{''}f_{l}^{'''}\right]\\&+2\beta\,\mathrm{Pr}\,Ec\,\mathrm{Re}\sum_{k=0}^{m-1}f_{m-1-k}^{''}\sum_{l=0}^{k}f_{k-l}^{''}\sum_{s=0}^{l}f_{l-s}^{''}f_{s}^{''}\\&+M^2\,\mathrm{Pr}\,Ec\left[f_{m-1}^{'}-E_1(1-\chi_m)\right]^2,\end{aligned}\tag{34}$$

$$\chi_m=\begin{cases}0, & m\le 1,\\ 1, & m>1.\end{cases}\tag{35}$$

The general solutions of the Eqs. (31)–(32) are

$$\begin{aligned}f_m(\eta)&=f_m^*(\eta)+C_1+C_2\exp(\eta)+C_3\exp(-\eta),\\\theta_m(\eta)&=\theta_m^*(\eta)+C_4\exp(\eta)+C_5\exp(-\eta),\end{aligned}$$

in which $f_m^*(\eta)$ and $\theta_m^*(\eta)$ denote the special solutions.

Convergence of the Derived Solutions

We note that the series solutions (33) and (34) contain the non-zero auxiliary parameters h_f and h_θ. These parameters are useful in adjusting and controlling the convergence. The h_f and h_θ −curves are plotted for 10^{th} order of approximation in Fig. 1 for the suitable ranges of the auxiliary parameters. Here the suitable values for h_f and h_θ are $-1.5\le h_f<-0.53$, $-1.35\le h_\theta<-0.4$. Furthermore, convergence of series solution is checked and shown in Table 1. Note that the series solutions converge at 26th order of approximation up to 6 decimal places.

Results and Discussion

This section illustrates the impact of physical parameters. The results are displayed graphically in the Figs. 2–20. The conclusions for flow field and other physical quantities of interest are drawn. The numerical values of the skin friction coefficient and local

Table 3. Numerical values of Nusselt number $\mathrm{Re}_x^{-1/2}Nu_x$ for different values of physical parameters.

α_1	α_2	β	S	M	E_1	Re	R_d	Pr	Ec	$\mathrm{Re}_x^{-1/2}Nu_x$
0.0	0.2	0.2	0.5	0.1	0.3	0.7	0.3	1.0	0.5	1.668
0.1										1.689
0.2										1.706
0.1	0.0	0.2	0.5	0.1	0.3	0.7	0.3	1.0	0.5	1.660
	0.1									1.674
	0.2									1.689
0.1	0.2	0.0	0.5	0.1	0.3	0.7	0.3	1.0	0.5	1.683
		0.3								1.691
		0.4								1.731
0.1	0.2	0.2	0.5	0.1	0.3	0.7	0.3	1.0	0.5	1.689
			0.6							1.805
			0.7							1.920
0.1	0.2	0.2	0.5	0.1	0.3	0.7	0.3	1.0	0.5	1.689
				0.5						1.669
				0.8						1.638
0.1	0.2	0.2	0.5	0.5	1.0	0.7	0.3	1.0	0.5	1.938
					1.5					1.889
					2.0					1.780
0.1	0.2	0.2	0.5	0.1	0.3	0.7	0.3	1.0	0.5	1.689
						1.0				1.668
						1.5				1.652
0.1	0.2	0.2	0.7	0.1	0.5	0.5	0.3	1.0	0.5	1.920
							0.4			1.991
							0.5			2.060
0.1	0.2	0.2	0.7	0.1	0.5	0.5	0.4	1.0	0.5	1.991
								1.1		2.109
								1.2		2.223
0.1	0.2	0.2	0.7	0.1	0.5	0.5	0.4	1.0	0.5	1.991
									0.6	1.938
									0.7	1.886

doi:10.1371/journal.pone.0083153.t003

Nusselt number are presented in the Tables 2 and 3 for various values of α_1, α_2, β, S, M, E_1, Re, R_d, Pr and Ec. Fig. 2 displays the effect of Hartman number M on velocity profile by keeping other physical parameter fixed. It is of interest to note that the velocity profile decreases with an increase in M whereas the boundary layer thickness reduces. Clearly by increasing magnetic force, the Lorentz force increases which cause resistance in the fluid flow and consequently the velocity profile decreases. Fig. 3 shows the influence of third grade parameter β on the velocity profile $f'(\eta)$. Here we noticed that the velocity increases near the wall with an increased β whereas it vanishes away from the wall. Figs. 4 and 5 illustrate the variation of second grade parameters α_1 and α_2 on the velocity profile $f'(\eta)$ respectively. It is observed that the velocity profile $f'(\eta)$ is an increasing function of α_1. The velocity profile also increases when α_2 is increased. Fig. 6 is plotted for the effects of the suction parameter A on the velocity profile $f'(\eta)$. The velocity profile decreases by increasing parameter A and further the boundary layer is also decreasing function of A. Fig. 7 is sketched for the influence of unsteadiness parameter S on the velocity profile. The velocity profile and the thermal boundary layer decreases for larger values of S. The behavior of Reynolds number Re on velocity profile is shown in Fig. 8. It is observed that the velocity profile decreases with an increase in Reynold number Re. The influence of electric parameter E_1 is shown in Fig. 9. This Fig explains that as the electric parameter E_1 increases, the velocity boundary layer increases near the plate with small rate but increases away from the stretching plate more rapidly. In fact the Lorentz force (arising due to the electric field acts like an accelerating force) reduces the frictional resistance which causes to shift the stream line away from the stretching sheet. Fig. 10 portrays the effects of magnetic parameter M on the temperature profile $\theta(\eta)$. It is depicted that temperature profile and thermal boundary layer thickness increase with an increase in magnetic parameter. Fig. 11 is the plot of temperature profile $\theta(\eta)$ for various values of third grade parameter β. The effect of third grade parameter β on $\theta(\eta)$ shows a decrease near the wall. The boundary layer thickness also decreases. Figs. 12 and 13 describe the effects of second grade parameters α_1 and α_2 on temperature profile $\theta(\eta)$. Fig. 12. depicts that the effect of second grade parameter α_1 is to reduce the temperature distribution in the boundary layer which results in thinning of the boundary layer thickness. Same behavior is shown in Fig. 13 for various values of

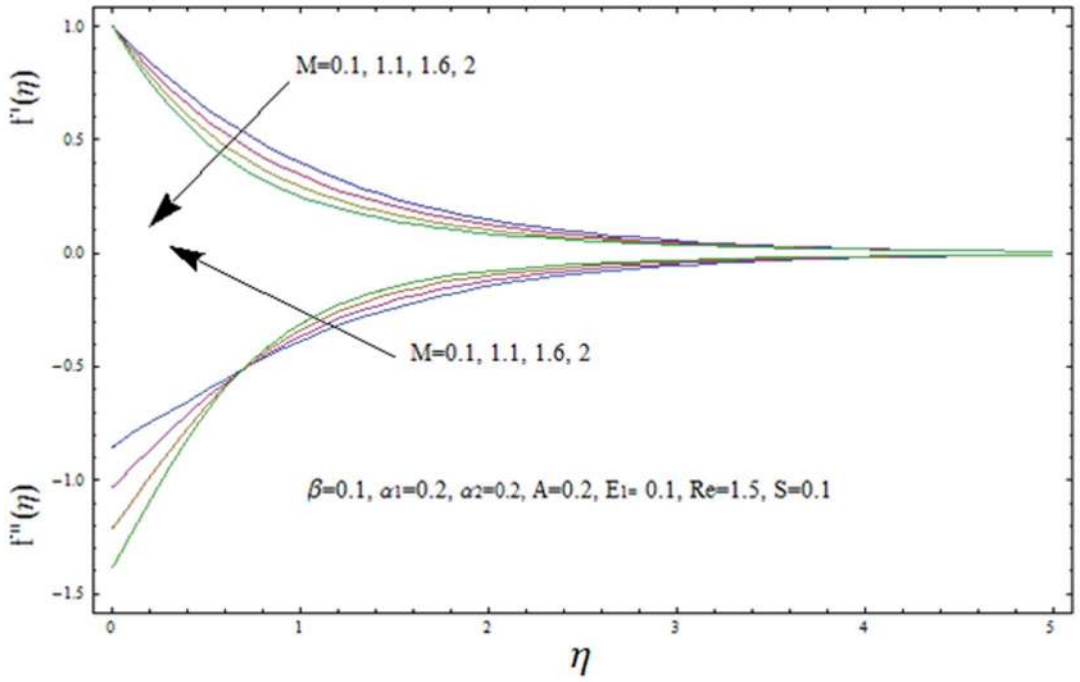

Figure 21. Variation of velocity f′(η) and shear stress f″(η) with η for several values of Hartman number M.
doi:10.1371/journal.pone.0083153.g021

α_2. The influence of suction parameter A and unsteadiness parameter S are analyzed in the Figs. 14 and 15. Here the temperature profile decreases with the increase of unsteadiness parameter S and the suction parameter A. Further the thermal boundary layer also decreases by increasing both the unsteadiness parameter S and the suction parameter A. Fig. 16 shows that the temperature profile and thermal boundary layer is decreasing function of Reynold number Re. The effects of thermal radiation parameter R_d on temperature is shown in Fig. 17. It is revealed that the radiation parameter R_d causes increase in the fluid temperature $\theta(\eta)$. On the other hand the thermal boundary layer thickness also increases. In Fig. 18 the influence of electric parameter E_1 on temperature profile is given. This Fig. depicts that the temperature profile and the boundary layer thickness

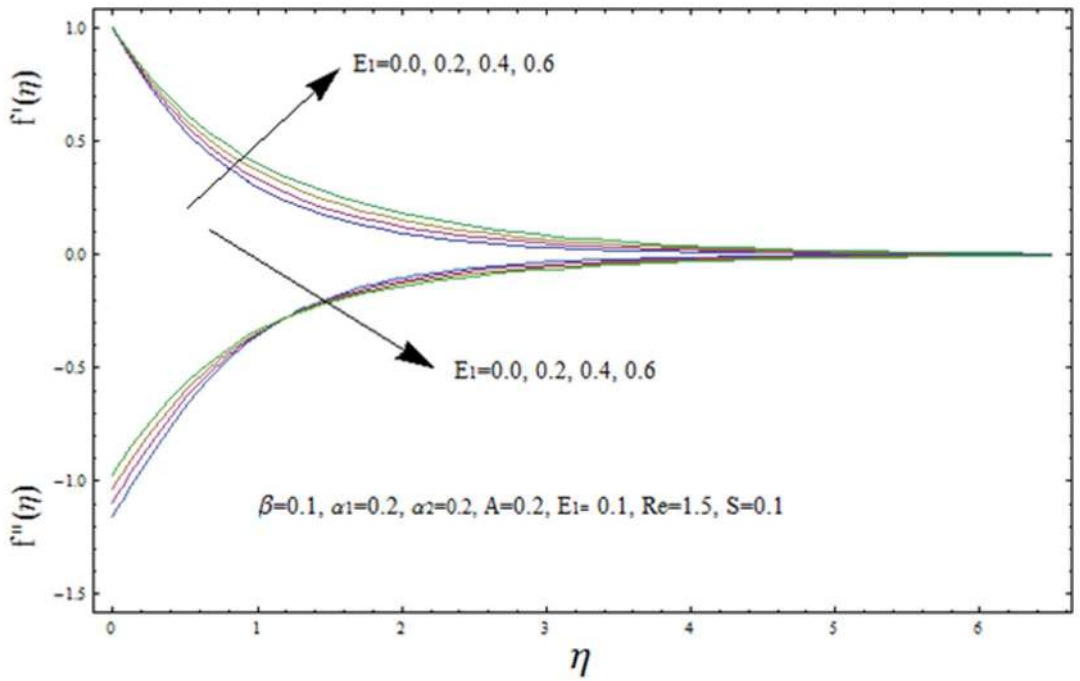

Figure 22. Variation of velocity f′(η) and shear stress f″(η) with η for several values of electric parameter E_1.
doi:10.1371/journal.pone.0083153.g022

increase with an increase of electric parameter E_1. Fig. 19. illustrates the effects of Prandtl number Pr on the temperature profile $\theta(\eta)$. Both the temperature and thermal boundary layer thickness are decreased by increasing Pr. We displayed the temperature field for various values of Eckert number Ec in Fig. 20. The effect of Eckert number is to increase the temperature boundary layer thickness due to the frictional heating. Fig. 21 shows the effects of Hartman number M on velocity $f'(\eta)$ and shear stress $f''(\eta)$. With the increase in M, the velocity field $f'(\eta)$ decreases near the wall and vanishes far away from the wall while shear stress $f''(\eta)$ has same behavior for larger values of Hartman number M. An opposite behavior is noted when $0 \leq \eta \leq 0.6$. Fig. 22 demonstrates the effects of electric parameter E_1 on velocity $f'(\eta)$ and shear stress $f''(\eta)$. It is worthmentioning to point out that velocity is increasing function of electric parameter E_1 near the wall whereas opposite behavior for shear stress is observed for $0 \leq \eta \leq 1$. The numerical values of skin friction coefficient for various physical parameters are shown in Table 2. Here the magnitude of skin friction coefficient increases with the increase of second grade parameters (α_1, α_2), third grade parameter β, unsteadiness parameter S, Hartman number M and Reynold number Re whereas it decreases with an increase in electric parameter E_1. Table 3 shows the effect of physical parameters on heat transfer characteristics at the wall $-\theta'(0)$. From this table, we observe that for large values of second grade parameters (α_1, α_2), third grade parameter β, unsteadiness parameter S, radiation parameter R_d and Prandtl number Pr the heat transfer coefficient at the wall $-\theta'(0)$ increases while it decreases for Hartman number M, Reynold number Re, electric parameter E_1 and Eckert number Ec.

Concluding remarks

The flow of third grade fluid and heat transfer in the presence of thermal radiation and Ohmic dissipation are examined. The graphs are prepared to study the influence of the pertinent flow parameters including the second grade parameter (α_1, α_2), third grade parameter β, unsteadiness parameter S, magnetic parameter M, electric field parameter E_1, Reynolds number Re, radiation parameter R_d, Prandtl number Pr and Eckert number Ec. The following observations hold:

- The effect of third grade parameter β is to increase the boundary layer thickness.
- The maximum velocity is attained for higher values of electric parameter E_1.
- Effect of suction parameter, unsteadiness parameter and Reynolds number on boundary layer thickness is similar in a qualitative sense.
- Effects of E_1 and Pr on temperature profile are quite opposite.
- The velocity field $f'(\eta)$ is decreasing function of Hartman number M.
- Magnitude of skin friction coefficient $\mathrm{Re}_x^{1/2} C_f$ is increasing function of α_1, α_2, β, S, M and Re.
- Electric parameter E_1 decreases the magnitude of skin friction coefficient.

Author Contributions

Conceived and designed the experiments: TH AS AA. Performed the experiments: TH AS AA. Analyzed the data: TH AS AA. Contributed reagents/materials/analysis tools: TH AS AA. Wrote the paper: TH AS AA.

References

1. Loureiroa JBR, Silva Freirea AP (2013), Asymptotic analysis of turbulent boundary-layer flow of purely viscous non-Newtonian fluids, Journal of Non-Newtonian Fluid Mechanics, 199: 20–28.
2. Keimanesha M, Rashidi MM, Chamkha AJ, Jafari R (2011), Study of a third grade non-Newtonian fluid flow between two parallel plates using the multi-step differential transform method, Computers and Mathematics with Applications, 62: 2871–2891.
3. Mustafa M, Hayat T, Obaidat S (2012), Stagnation-point flow and heat transfer of a Casson fluid towards a stretching sheet, Z Naturforsch 67: 70–76.
4. Abbasbanday S, Hayat T (2011), On series solution for unsteady boundary layer equations in a special third grade fluid, Commun Nonlinear Sci Numer Simulat, 16: 3140–3146.
5. Mahmoud AAM (2011), Slip velocity effect on a non-Newtonian power-law fluid over a moving permeable surface with heat generation, Mathematical and Computer Modelling, 54: 1228–1237.
6. Hayat T, Asad S, Qasim M, Hendi AA (2012), Boundary layer flow of a Jeffrey fluid with convective boundary conditions, Int J Numer Meth Fluids 69: 1350–1362.
7. Renardy M, Wang X (2012), Boundary layer for the upper convected Maxwell fluid, J Non-Newtonian Fluid Mech, 189–190: 14–18.
8. Ramzan M, Farooq M, Alsaedi A, Hayat T (2013), MHD three dimensional flow of couple stress fluid with Newtonian heating, Eur Phys J Plus, 128: 49.
9. Shafiq A, Nawaz M, Hayat T, Alsaedi A (2013), Magnetohydrodynamic axisymmetric flow of a third grade fluid between two porous disks, Brazilian J Chem Engineer 30 (3).
10. Sahoo B, Labropulu F (2012), Steady Homann flow and heat transfer of an electrically conducting fluid, Computers Math Appli, 63: 1244–1255.
11. Rana P, Bhargava R (2012) Flow and heat transfer of a nanofluid over a nonlinearly stretching sheet: A numerical study, Commun Nonlinear Sci Num Simu 17: 212–226.
12. Bhattacharyya K, Uddin MS, Layeka GC, Ali Pk W (2011), Unsteady helical flows of Oldroyd-B fluids, Comm Nonlinear Sci Num Simu, 16: 1378–1386.
13. Makinde OD, Aziz A (2011) Boundary layer flow of a nanofluid past a stretching sheet with a convective boundary condition, Int J Thermal Sciences, 50: 1326–1332.
14. Mandal IC, Mukhopadhyay S (2013) Heat transfer analysis for fluid flow over an exponentially stretching porous sheet with surface heat flux in porous medium, Ain Shams Engineering Journal 4: 103–110.
15. Hayat T, Iqbal Z, Mustafa M (2012) Flow of a second grade fluid over a stretching surface with Newtonian heating, Journal of Mechanics, 28(1): 209–216.
16. Sajid M, Hayat T (2008), Influence of thermal radiation on the boundary layer flow due to an exponentially stretching sheet, Int Commun Heat Mass Transfer, 35: 347–356.
17. Bhattacharyya K (2013) Heat transfer analysis in unsteady boundary layer stagnation point flow towards a shrinking/stretching sheet, Ain Shams Eng Journal, 4: 259–264.
18. Mukhopadhyay S (2013) MHD boundary layer flow and heat transfer over an exponentially stretching sheet embedded in a thermally stratified medium, Alexandria Eng Journal, 52: 259–265.
19. Hussain M, Ashraf M, Nadeem S, Khan M (2013) Radiation effects on the thermal boundary layer flow of a micropolar fluid towards a permeable stretching sheet, J Fran Institute 350: 194–210.
20. Rashidi MM, Mohimanian Pour SA, Abbasbandy S (2011) Analytic approximate solutions for heat transfer of a micropolar fluid through a porous medium with radiation, Comm Nonlinear Sci Numer Simulation, 16: 1874–1889.
21. Turkyilmazoglu M (2011) Exact solutions for the incompressible viscous magnetohydrodynamic fluid of a rotating disk flow. Int J Nonlinear Mech 46: 306–311.
22. Hayat T, Nawaz M (2011) Soret and Dufour effects on the mixed convection flow of a second grade fluid subject to Hall and ion-slip currents, Int J Numer Meth Fluids, 67: 1073–1099.
23. Ahmad K, Nazar R (2010) Unsteady magnetohydrodynamic mixed convection stagnation point flow of a viscoelastic fluid on a vertical surface, JQMA, 6 (2): 105–117
24. Pal D, Mondal H (2010) Hydromagnetic non-Darcy flow and heat transfer over a stretching sheet in the presence of thermal radiation and ohmic dissipation, Commun Nonlinear Sci Numer Simulat, 15: 1197–1209.
25. Abel MS, Sanjayanand E, Nandeppanavar MM (2008) Viscoelastic MHD flow and heat transfer over a stretching sheet with viscous and Ohmic dissipations. Commun Nonlinear Sci Numer Simulat, 13: 1808–1821.
26. Hayat T, Qasim M (2011) Radiation and Magnetic field effects on the unsteady mixed convection flow of a second grade fluid over a vertical stretching sheet, Int J Numer Meth Fluids, 66: 820–832.
27. Olanrewaju PO (2012) Effects of internal heat generation on hydromagnetic non-Darcy flow and heat transfer over a stretching sheet in the presence of

thermal radiation and ohmic dissipation, World Applied Sciences Journal, 16: 37–45.
28. Elbashbeshy EMA, Emam TG, Abdelgaber KM (2012), Effects of thermal radiation and magnetic field on unsteady mixed convection flow and heat transfer over an exponentially stretching surface with suction in the presence of internal heat generation/absorption, Journal of the Egyptian Mathematical Society 20: 215–222.
29. Rashidi MM, Abelman S, Mehr NF (2013) Entropy generation in steady MHD flow due to a rotating disk in a nanofluid, Int J Heat Mass Transfer, 62: 515–525.
30. Motsa SS, Sibanda P, Awad FG, Shateyi S (2010) A new spectral homotopy analysis method for the MHD Jeffery Hamel problem, Computers and Fluids, 39: 1219–1225.
31. Liao SJ (2009) Notes on the homotopy analysis method: Some definitions and theorems, Comm Nonlinear Sci Num Simu 14: 983–997.
32. Liao SJ (2012) Homotopy analysis method in nonlinear differential equations, Springer & Higher Education Press.
33. Hassan HN, El-Tawil MA (2012) A new technique of using homotopy analysis method for second order nonlinear differential equations, Appl Math Comput 219: 708–728.
34. Bataineh AS, Noorani MSM, Hashim I (2009) On a new reliable modification of homotopy analysis method, Commn Nonlinear Sci Numer Simulation, 14: 409–423.
35. Rashidi MM, Ali M, Freidoonimehr N, Nazari F (2013) Parametric analysis and optimization of entropy generation in unsteady MHD flow over a stretching rotating disk using artificial neural network and particle swarm optimization algorithm, Energy, 497–510.
36. Ellahi R, Shivanian E, Abbasbandy S, Rahmanb SU, Hayat T (2012) Analysis of steady flows in viscous fluid with heat/mass transfer and slip effects, Int J Heat Mass Transfer, 55: 6384–6390.
37. Hayat T, Shafiq A, Nawaz M, Alsaedi A (2012) MHD axisymmetric flow of third grade fluid between porous disks with heat transfer, Appl Math Mech 33(6): 749–764.
38. Hayat T, Farooq M, Alsaedi A, Iqbal Z (2013) Melting heat transfer in the stagnation point flow of Power-Eyring fluid. J Thermophys Heat Trans 27: 761–766.
39. Ramzan R, Farooq M, Alsaedi A, Hayat T (2013) MHD three dimensional flow of couple stress fluid with Newtonian heating. Eur Phys J Plus, 128: 49.
40. Turkyilmazoglu M (2012) Solution of the Thomas–Fermi equation with a convergent approach, Commun Nonlinear Sci Numer Simulat, 17: 4097–4103.
41. Sparrow EM, Cess RD (1978) Radiation Heat Transfer. Washington: Hemisphere.
42. Raptis A (1998) Radiation and free convection flow through a porous medium. Int Commun Heat Mass Transf, 25: 289–295.